THE PROTON STRUCTURE FUNCTION AT MEDIUM Q^2 AT HERA

TH. NAUMANN
FOR THE H1 AND ZEUS COLLABORATIONS AT HERA
Deutsches Elektronen-Synchrotron, DESY Zeuthen,
Platanenallee 6, D-15738 Zeuthen, Germany, E-mail: naumann@ifh.de

We present preliminary measurements of the proton structure function in deep inelastic *ep* scattering by the experiments H1 and ZEUS at HERA together with QCD fits to the NLO DGLAP equations. The extraction of the longitudinal structure function F_L from the inclusive cross section by the H1 experiment with two different methods is discussed. Both experiments extracted the charm structure function F_2^c and observed a behaviour similar to the inclusive structure function F_2. Finally, the results of different measurements of the gluon momentum distribution by H1 and ZEUS are given.

1 Introduction

The measurement of the inclusive neutral current deep inelastic scattering (DIS) cross section and the extraction of the proton structure functions are one of the major physics tasks at the HERA accelerator. They help to understand the structure of the proton and to precisely test QCD as the gauge theory of strong interactions.

In section 2 we describe preliminary measurements of the inclusive DIS cross section and the structure function F_2 at HERA. The results of QCD fits to the NLO DGLAP equations are given in section 3. The behaviour of the longitudinal structure function F_L should be described by the same set of parton distribution functions, in particular the gluon distribution, and within the same QCD framework as the inclusive structure function F_2. In section 4 we present two approaches used by the H1 experiment to extract F_L. Section 5 describes the extraction of the charm structure function F_2^c and section 6 the measurement of the gluon distribution of the proton.

2 Measurement of the Inclusive Cross Section

For $Q^2 \ll M_Z^2$ the inclusive NC lepton-nucleon DIS cross section can be written as follows:

$$\frac{d^2\sigma(lN)}{dxdQ^2} = \frac{2\pi\alpha^2}{Q^4 x}[Y_+ F_2(x,Q^2) - y^2 F_L(x,Q^2)]\ (1+\delta_r). \tag{1}$$

Here, Q^2 is the four-momentum transfer squared between the incoming and the scattered lepton, x the parton momentum fraction in the proton, y the inelasticity, δ_r are the radiative corrections and $Y_+ = 1 + (1-y)^2$.

From this expression the so-called reduced cross section σ_r can be defined:

$$\sigma_r = \frac{d^2\sigma}{dxdQ^2}\frac{Q^4 x}{2\pi\alpha^2 Y_+} = F_2(x,Q^2) - \frac{y^2}{Y_+}F_L(x,Q^2) \tag{2}$$

Since $F_L = F_2 - 2xF_1 \geq 0$ so that $F_2 \geq F_L$ and $y^2/Y_+ < 1$ the cross section is always dominated by F_2. The longitudinal structure function F_L is best measureable at high y.

The H1 and ZEUS detectors are described in detail in refs. 1 and 2. During 1996 and 97 H1 collected a luminosity of 15 pb^{-1} at $Q^2 > 10$ GeV^2 and ZEUS a luminosity of 27 pb^{-1} at $Q^2 > 27$ GeV^2 with a DIS trigger setup. This leads to a statistical precision of about 1% for the chosen binning.

Table 1. Main sources of systematic errors and their effect on the cross section measurement accuracy.

source	error [%]
positron identification	1-2
vertex efficiency	1-2
trigger efficiency	0.5 - 1
photoproduction background	$<$ 8-10 at high y
radiative corrections	1-2
HERA luminosity	1.5

The typical size of the systematic errors is summarized in Table 1. The electron energy scale was calibrated by H1 with the double angle method and is known to 0.5%. The hadronic energy scale was calibrated with the p_t balance and is known to 3-4%. The angle of the scattered positron was measured by the H1 backward tracking detectors with a precision of 0.5 mrad . The amount of non - e-p background was estimated to be below 1%. The total systematic errors are mostly below 4% reaching 8 and 10% at the highest y for H1 and ZEUS, resp.

Fig. 1 shows the x dependence of the proton structure function F_2 as measured by the ZEUS experiment [3] in bins of Q^2 . The structure function strongly increases towards low x. The steepness of the x dependence which can be expressed as $F_2(x) \sim x^{-\lambda}$ is seen to increase with Q^2 .

3 QCD Fits

Both experiments performed QCD fits to the NLO DGLAP equations in the $\overline{MS}$ renormalization scheme. The input parton distributions at the starting scale Q_0^2 were parametrized as follows:

$$xq(x) = A_q x^{B_q}(1-x)^{C_q}(1 + D_q x + E_q\sqrt{x}) \tag{3}$$

where $q = g, u_v, d_v, S$ denotes the gluon, valence and sea quark distributions and $S = \overline{u} = \overline{d}$. The momentum sum rule $\int_0^1 dx\, x(g+\Sigma) = 1$ fixes the sea normalization A_S while the quark counting rules $\int_0^1 dx\, u_v = 2$ and $\int_0^1 dx\, d_v = 1$ fix the normalizations A_u and A_d of the valence quark distributions.

The fits were done in the fixed flavor number scheme with three massless flavors u,d,s. The contribution of strange quarks at Q_0^2 was assumed to be s = 0.2 $(\bar{u} + \bar{d})$. The contribution from the charm structure function F_2^c was added according to the

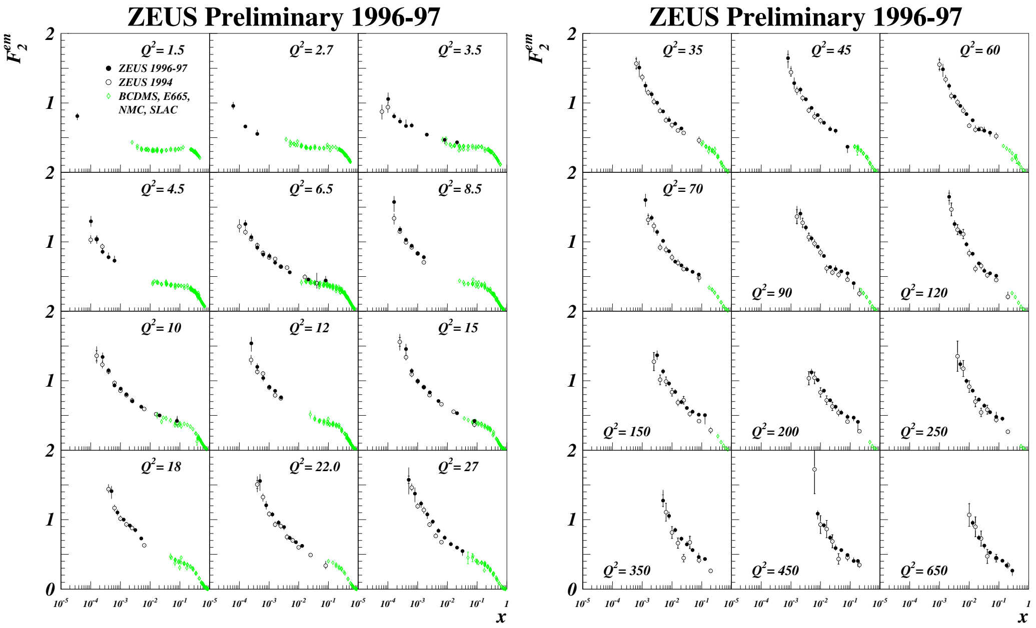

Figure 1. The x dependence of the proton structure function F_2 as measured by the ZEUS experiment in bins of Q^2 .

NLO calculation of the photon-gluon fusion process [4]. The mass of the charm quark was set to $m_c = 1.5$ GeV. The strong coupling constant was evolved according to NLO QCD with the constraint $\alpha_s(M_Z^2) = 0.118$.

Two independent programs were used by the ZEUS [5] and H1 [6] experiments to perform the QCD evolution of tbe parton densities. Correlated systematic experimental errors were taken into account by varying the error source within one standard deviation and refitting the modified data. Theoretical errors were taken into account varying the strong coupling constant by $\delta\alpha_s = 0.005$, the charm quark mass by $\delta m_c = 0.2$ GeV, the strange sea fraction by 0.1, and the starting point of the evolution Q_0^2.

BCDMS [7] and NMC [8] proton and deuteron data were used in the fits. In order to reduce non-perturbative effects data with $x > 0.5$ were excluded from the fits at $Q^2 < 15$ GeV^2. The ZEUS experiment used data with $Q^2 > 1$ GeV^2 and an evolution starting scale $Q_0^2 = 7$ GeV^2. H1 included data with $Q^2 > 2$ GeV^2 and a starting scale $Q_0^2 = 2$ GeV^2.

Fig. 2 shows the Q^2 dependence of the proton structure function F_2 for low and medium values of x as measured by the H1 experiment [9] together with the QCD fit. As can be seen the NLO DGLAP equations are able to correctly describe the data down to $Q^2 \sim 2$ GeV^2. At low x the logarithmic derivative of the structure function is proportional to the gluon density: $dF_2/d\ln Q^2 \sim \alpha_s P_{qg} \otimes xg$. This means that the scaling violations are determined by the gluon distribution. Since the scaling violations strongly increase towards low x we expect a strong increase of the gluon

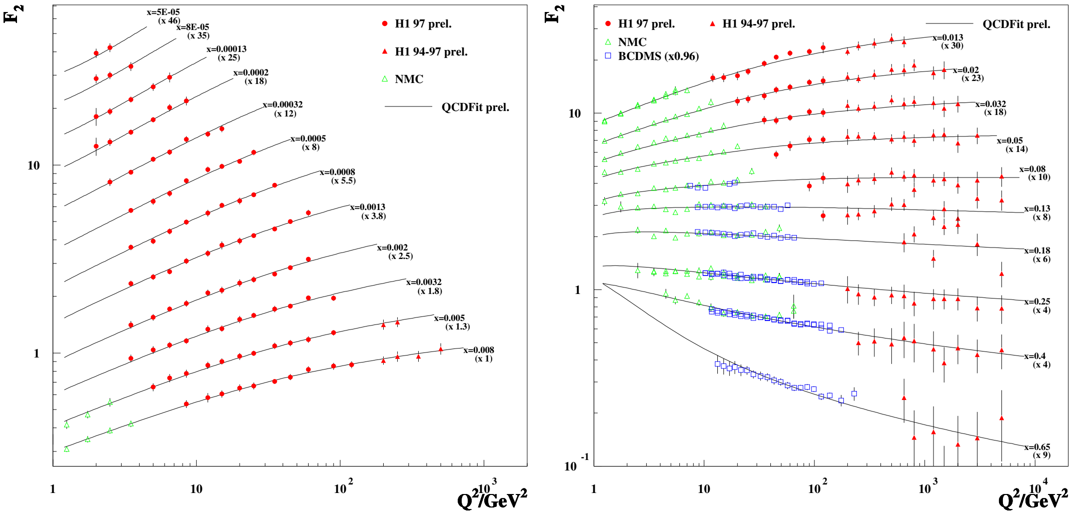

Figure 2. The Q^2 dependence of the proton structure function F_2 for low and medium values of x as measured by the H1 experiment together with the H1 QCD fit.

distribution at low x. At $x > 0.005$ Fig. 2 also shows that HERA and fixed target experiments agree well. Scaling is observed at $x \sim 0.1$ up to $Q^2 = 5000$ GeV^2.

4 Determination of the Longitudinal Structure Function F_L

From Eq. (2) we get the expression $F_L = Y_+/y^2(F_2 - \sigma_r)$ for the longitudinal structure function F_L. The H1 experiment performed a QCD fit to F_2 in the region $y < 0.35$ where F_L is negligible and extrapolated this fit to high y. Fig. 3 shows that at low x $F_2(x)$ significantly deviates from σ_r. This difference allows to extract F_L by subtracting the measured reduced cross section from the QCD fit.

Another approach used by H1 is to derive the reduced cross section at fixed Q^2 :

$$\frac{\partial \sigma_r}{\partial \ln y} = -\frac{\partial F_2}{\partial \ln x} - F_L \cdot 2y^2 \cdot \frac{2-y}{Y_+^2} + \frac{\partial F_L}{\partial \ln x} \cdot \frac{y^2}{Y_+} \tag{4}$$

A straight line fit to $\partial\sigma_r/\partial \ln y = A \ln y + B$ was done in the region $y < 0.2$ where F_L is small. The linearity was checked with the QCD fit and small differences put to the error. This method allows to access lower Q^2 than the subtraction method.

In Fig. 4 the results of the two methods used by H1 to determine F_L are shown. The longitudinal structure functions determined by both methods are consistent although they use different aspects of the behaviour of F_2 and F_L . The shaded band represents the F_L prediction from the parton distributions determined with the QCD fit which agrees with the measurement. The full line illustrates the extreme

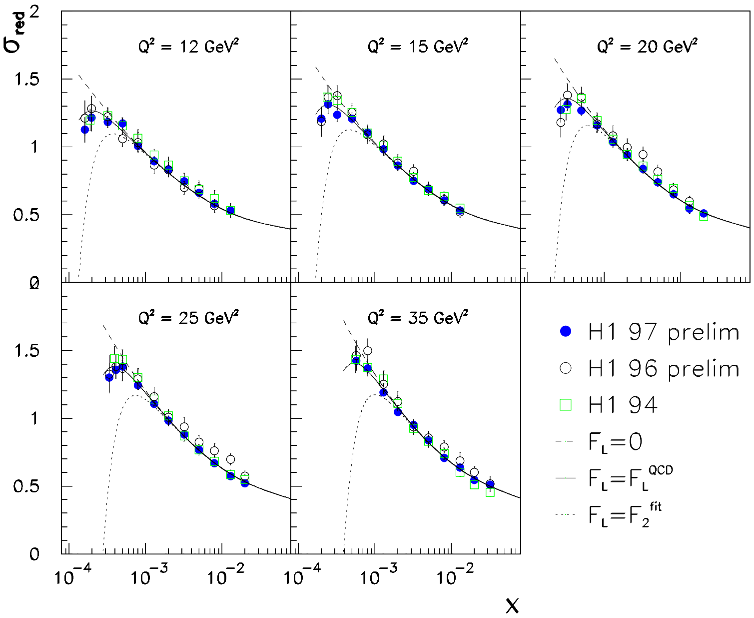

Figure 3. Measurement of the reduced DIS cross section σ_r by the H1 experiment together with QCD predictions under different assumptions on F_L. At low x or $y > 0.5$ the cross section significantly deviates from the assumption F_L=0 which allows to extract F_2 .

case that F_L saturates the cross section. Irrespective of these results a direct F_L measurement should be done by varying the HERA beam energies.

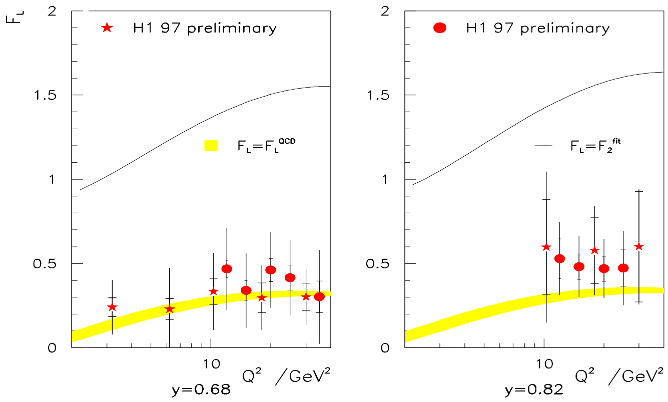

Figure 4. Determination of the longitudinal structure function F_L with the subtraction method (full points) and the derivative method (stars). The shaded band represents the F_L prediction from the parton distributions determined with the NLO QCD fit.

5 Extraction of the Charm Structure Function F_2^c

The charm quark was tagged by the small mass difference $\Delta m_{D^*-D} = 142$ MeV between the D^* and the D mesons in the decay chain $D^* \to D^0\pi_{slow} \to K\pi\pi_{slow}$. To extract F_2^c the fragmentation functions of a charm quark into a D meson and an extrapolation to the full η and p_t range of the D^* by up to factor 4 are needed. ZEUS [10] also used the semileptonic decay mode. Neglecting a small F_L^c contribution the final extraction of F_2^c is similar to the F_2 measurement.

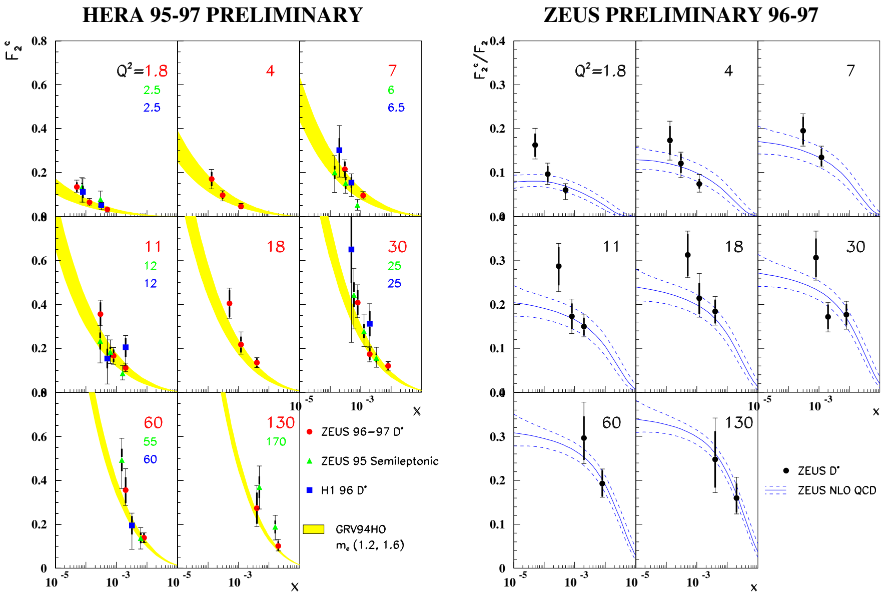

Figure 5. The x dependence of the charm structure function F_2^c of the proton as measured by the H1 and ZEUS experiments (left) and the charm fraction of the proton F_2^c/F_2 (right) together with predictions from the ZEUS QCD fit.

The results of ZEUS [10] and H1 [11] are shown in Fig. 5. Both experiments now reach a precision of $\delta F_2^c/F_2^c$ = 15-20%. Fig. 5 also shows that the charm content of the proton grows from 10 to 25% between Q^2 =1.8 and 130 GeV^2. The charm structure function exhibits the same steep rise towards low x as the total F_2. It also agrees with predictions from QCD analyses of the full F_2. Both structure functions are determined by the same gluon distribution.

6 Measurement of the Gluon Momentum Distribution

Assuming photon-gluon fusion as the main process for inclusive DIS charm production the gluon momentum distribution $xg(x)$ can be measured from the differential charm production cross section. The momentum fraction x_g of the gluon is determined from the kinematics of the scattered electron and from the transverse momentum p_t and the total $(E - p_z)$ of the D* meson. The true x_g is iteratively unfolded using a NLO heavy quark DIS QCD Monte Carlo program and the Peterson fragmentation functions. Fig. 6 shows that the gluon obtained from the DIS D^* cross section agrees with the gluon from D^* photoproduction and also with the prediction from the QCD fit to the inclusive cross section.

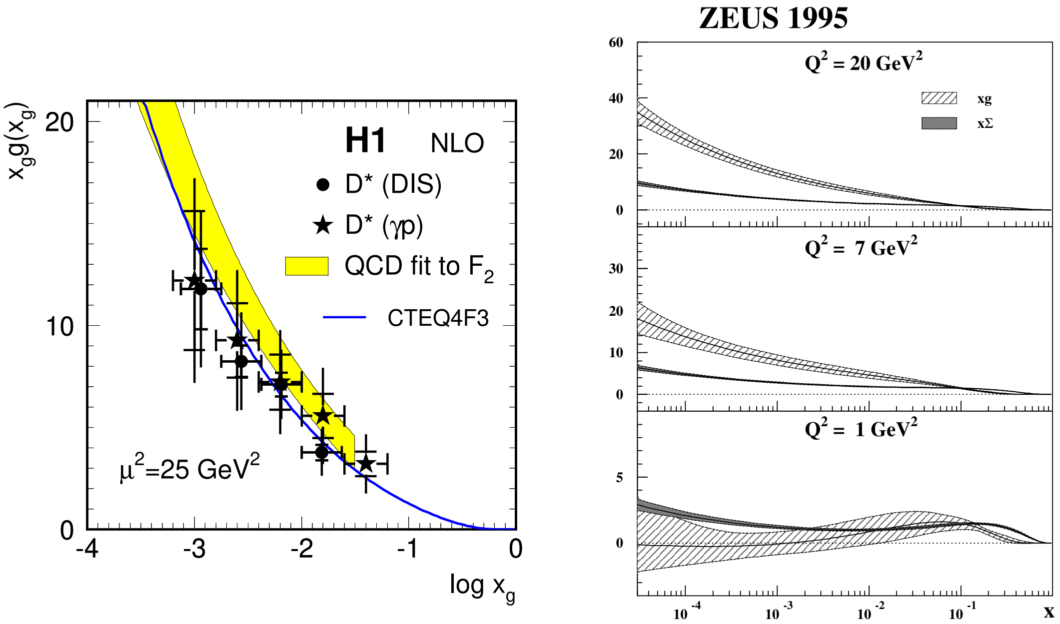

Figure 6. Left: The gluon momentum distribution $xg(x)$ determined by H1 from the inclusive production of D^* mesons. Right: The gluon momentum distribution $xg(x)$ obtained by ZEUS from a NLO QCD fit to the structure function F_2 for $Q^2 = 1,7,20$ GeV^2. The error bands correspond to the quadratic sum of all errors considered in the fit: statistical, experimental and theoretical systematic, and parametrization errors.

Fig. 6 shows the gluon momentum distribution $xg(x)$ obtained by ZEUS from the NLO QCD fit to F_2 described above together with the singlet distribution $x\Sigma(x)$. At $x = 5 \cdot 10^{-4}$ and $Q^2 = 20$ GeV^2 the error of the gluon distribution could be reduced to 10%. It is interesting to see that the data are best fitted by a valence-like gluon distribution at $Q^2 = 1$ GeV^2 and that QCD seems to work at 1 GeV^2. With rising Q^2 the gluon evolves much faster than the sea. At $Q^2 \gg 1\, GeV^2$ the gluon determines the sea and hence F_2 .

7 Summary

A precision of a few percent for the preliminary measurements of the proton structure function F_2 at medium Q^2 was reached by the ZEUS and H1 experiments at HERA. A steep rise of the structure function towards low x is observed which can be parametrized as $F_2(x) \sim x^{-\lambda}$. The scaling violations $dF_2/d\ln Q^2 \sim \alpha_s P_{qg} \otimes xg$

which are determined by the gluon distribution strongly grow towards low x. QCD fits to the NLO DGLAP equations show that QCD works over more than 4 orders of magnitude in the range $2 \cdot 10^{-5} < x < 0.7$ and $1 < Q^2 < 30.000$ GeV^2.

The longitudinal structure function F_L was extracted by H1 with two methods which agree with each other and with QCD.

The charm structure function F_2^c was measured by both experiments. It exhibits the same rise with falling x as the inclusive structure function F_2. The ratio F_2^c/F_2 grows from 10 to 25% from $Q^2 = 1.8$ to 130 GeV^2. F_2^c agrees with the QCD prediction obtained from the scaling violations of F_2 .

The gluon momentum distribution $xg(x)$ was determined from the F_2 scaling violations and from the charm cross section. Starting from a valence-like behaviour at $Q^2 = 1$ GeV^2 it exhibits a fast Q^2 evolution leading to a steep increase in x at $Q^2 \gg 1$ GeV^2.

Summarizing, the proton structure functions F_2, F_L, and F_2^c are all well described within the framework of perturbative QCD by the NLO DGLAP equations and by the same gluon momentum distribution $xg(x)$. Both collaborations are finalizing their data analyses for final publications.

References

1. H1 Collaboration, I. Abt *et al.*, *Nucl. Instrum. Methods* A **386**, 310 (1997) and *Nucl. Instrum. Methods* A **386**, 348 (1997)
2. ZEUS Collaboration, M.Derrick *et al.*, *Phys. Lett.* B **293**, 465 (1992)
3. ZEUS Collaboration, XXIX Int. Conf. on High Energy Physics, Vancouver, Canada, July 1998, paper 769.
4. S. Riemersma, J. Smith and W. van Neerven, *Phys. Lett.* B **347**, 143 (1995)
5. M.Botje, Workshop on Deep Inelastic Scattering at Low x, Zeuthen, April 1998, unpublished.
6. C. Pascaud and F. Zomer, LAL preprint, LAL/95-05 (1995)
7. BCDMS Collaboration, A.C. Benvenuti *et al.*, *Phys. Lett.* B **223**, 485 (1989); CERN preprint CERN-EP/89-06.
   M. Virchaux and A. Milzstajn, *Phys. Lett.* B **274**, 221 (1992)
8. NMC Collaboration, M. Arneodo *et al.*, *Nucl. Phys.* B **483**, 3 (1997)
9. H1 Collaboration, XXIX Int. Conf. on High Energy Physics, Vancouver, Canada, July 1998, paper 534
10. ZEUS Collaboration, XXIX Int. Conf. on High Energy Physics, Vancouver, Canada, July 1998, papers 768 and 772
11. H1 Collaboration, DESY preprint DESY 98-204, subm. to *Nucl. Phys.* B
12. ZEUS Collaboration, DESY preprint DESY 98-121, accepted by *Eur.Phys.J.*